A Purified *Drosophila* Septin Complex Forms Filaments and Exhibits GTPase Activity

Christine M. Field,* Omayma Al-Awar,§ Jody Rosenblatt,* Mei Lie Wong,* Bruce Alberts,* and Timothy J. Mitchison‡

*Department of Biochemistry and Biophysics, ‡Department of Cellular and Molecular Pharmacology, University of California at San Francisco, California 94143-0448; and §Department of Biology, University of North Carolina, Chapel Hill, North Carolina 27599

Abstract. Septin proteins are necessary for cytokinesis in budding yeast and *Drosophila* and are thought to be the subunits of the yeast neck filaments. To test whether septins actually form filaments, an immunoaffinity approach was used to isolate a septin complex from *Drosophila* embryos. The purified complex is comprised of the three previously identified septin polypeptides Pnut, Sep2, and Sep1. Hydrodynamic and sequence data suggest that the complex is composed of a heterotrimer of homodimers. The complex copurifies with one molecule of bound guanine nucleotide per septin polypeptide. It binds and hydrolyzes exogenously added GTP. These observations together with conserved sequence motifs identify the septins as members of the GTPase superfamily. We discuss a model of filament structure and speculate as to how the filaments are organized within cells.

CYTOKINESIS involves the concerted activity of cytoskeletal and membrane systems to create two cells from one. Despite differences in morphology and apparent mechanism, yeast cells and animal cells appear to use a similar set of proteins to accomplish this step in cell division. Actin and the recently identified septin proteins are required in both systems (reviewed by Sanders and Field, 1994, and Longtine et al., 1996). The septins are a homologous family of proteins identified in budding and fission yeast (Haarer and Pringle, 1987; Ford and Pringle, 1991; Kim et al., 1991; Pringle, J., personal communication), *Drosophila* (Neufeld and Rubin, 1994; Fares et al., 1995), mammals, (Kato, 1990; Nottenburg et al., 1990; Kumar et al., 1992; Nakatsuru et al., 1994), and *Xenopus* (Glotzer, M., and T. Hyman, personal communication). They appear to be involved in cytokinesis or septum formation, perhaps including the regulation of plasma membrane–cortical cytoskeleton interactions and playing a more general role in cell-surface organization. The four original septin family members, encoded by *CDC3*, *CDC10*, *CDC11*, and *CDC12*, were first identified in budding yeast on the basis of mutations affecting the cell division cycle (Hartwell, 1971). The phenotypes of all four mutations are indistinguishable, with defects in bud morphogenesis, cytokinesis, and the localization of chitin deposition. In *Drosophila*, a mutation in the septin gene *peanut* (*pnut*) also exhibits a phenotype consistent with a cytokinesis defect (Neufeld and Rubin, 1994).

The four yeast genes were cloned and sequenced by Pringle and co-workers (These sequence data are available from EMBL/GenBank/DDBJ under accession numbers L16548–L16551). Their predicted amino acid sequences revealed that they encode homologous polypeptides and first established the septin family. The sequences of all known septins contain a P loop nucleotide–binding consensus sequence (Saraste et al., 1990) near the NH_2 terminus and additional motifs (Flescher et al., 1993; Nakatsuru et al., 1994) homologous to the consensus sequences that define the GTPase superfamily (Bourne et al., 1991). In addition, most but not all of the septin polypeptides contain predicted coiled-coil domains of 36–90 amino acids near their COOH termini. Although the septin family is broadly conserved (30–73% identical), there is generally not a close one-to-one correspondence between individual polypeptides in different organisms. (See Neufeld and Rubin, 1994, Fares et al., 1995, and Longtine et al., 1996 for multiple sequence alignments of septins from various organisms).

Studies of wild-type and mutant yeast by EM and immunofluorescence have led to the hypothesis that the septin polypeptides are the major structural components of the 10-nm "neck filaments" found encircling the mother bud neck (Byers, 1981; Byers and Goetsch, 1976; Ford and Pringle, 1991; Haarer and Pringle, 1987; Kim et al., 1991) Assembly of the four septin proteins appears to be interdependent, since all four septin polypeptides disappear

Please address all correspondence to C.M. Field, Department of Biochemistry and Biophysics, University of California, San Francisco, CA 94143-0448. Tel.: (415) 476-4581. Fax: (415) 476-0806. E-mail: cfield@socrates.ucsf.edu

from the bud neck when temperature-sensitive mutants of any septin gene are shifted to the nonpermissive temperature, as judged by immunofluorescence (Haarer and Pringle, 1987; Kim et al., 1991).

These studies imply that there is a functional relationship between the septin polypeptides and the neck filaments, but they do not prove that the septins themselves polymerize. It is also unclear whether the septins in other organisms are associated with higher order structures such as the neck filaments of budding yeast. Important outstanding questions include: (*a*) Are the septin proteins the principal structural components of the yeast neck filaments, or are some of them regulatory subunits or accessory proteins? (*b*) Can septins form filaments in vitro and do they do so in other organisms? (*c*) Do septins bind guanine nucleotide, as suggested by the GTPase consensus sequences, and if so, with what functional consequence? (*d*) How are the spatial organization of the septins and their assembly into higher order structures controlled during the cell cycle? (*e*) What is the function of the septins? In this study, we use biochemical techniques to purify and analyze a complex of septin polypeptides from *Drosophila* embryos. This has allowed the first three questions to be addressed directly. The results also provide a basis for speculation about the control of septin filament formation and spatial organization inside the cells.

Materials and Methods

Preparation of Antiseptin Antibodies

The anti-Pnut antibody (referred to as KEKK antibody) was raised against the COOH-terminal 14 amino acids of the *Drosophila* Pnut polypeptide (Neufeld and Rubin, 1994) with the addition of an acetylated NH_2-terminal cysteine to facilitate coupling (Ac-CNVDGKKEKKK-KGLF). Preparation of keyhole limpet hemocyanin conjugates and affinity purification were performed as described in Sawin et al. (1992). The antibodies were generated in rabbits by Berkeley Antibody Company (Richmond, CA). Western blots were performed as described (Kellogg et al., 1989) using alkaline phosphatase–conjugated secondary antibodies.

To prepare antibodies specific for Sep2, 981 bp encoding the carboxyl-terminal 327 amino acids (These squence data are available under EMBL/GenBank/DDBJ accession number U28966) were amplified by PCR from a cDNA clone. The amplified product was inserted into the pATH1 vector (Koerner et al., 1991), resulting in a TrpE–Sep2 fusion, and into the pGex-2T vector (Smith and Johnson, 1988), resulting in a glutathione *S*-transferase (GST)[1]–Sep2 fusion. *Escherichia coli* cells carrying the fusion plasmids were induced and the insoluble fractions were isolated. In both cases, these fractions were highly enriched (>95% of total protein) for proteins of the sizes predicted for the desired fusions, as judged by SDS-PAGE. The GST–Sep2–insoluble fraction was injected into rabbits using standard protocols (Cocalico Biologicals, Reamstown, PA). Samples of both insoluble fractions were electrophoresed on SDS-PAGE and transferred electrophoretically to nitrocellulose membranes for use in affinity purification (Pringle et al., 1989). Sep2-specific antibodies were purified in two steps, first on a blot containing TrpE–Sep2, and then on a blot containing GST–Sep2.

Antibodies specific for Sep1 were prepared as described (Fares et al., 1995).

Extract Preparation

Extracts of 0–4-h-old embryos were prepared by modifications of the procedure of Miller et al. (1991). The extraction buffer consisted of 5 mM Tris-HCl, pH 7.9, 0.5 mM Na_3 EDTA, 0.5 mM Na_3 EGTA, 0.1% NP-40 and protease inhibitors (10 μg/ml each of leupeptin, aprotinin, and pepstatin). 5 vol of this buffer was added per gram of embryos. PMSF was added to 1 mM. After a 20-min spin at 10,000 *g*, the supernatant was brought to 50 mM Tris-HCl, pH 7.9, 1 mM DTT, and was centrifuged for 1 h at 100,000 *g*. This high speed supernatant (HSS) was used for complex isolation. Under these conditions, ~50% of the Pnut protein sedimented in the first spin and very little in the second spin, as detected by Western blotting.

Complex Isolation

Affinity-purified KEKK antibody was adsorbed to protein A–agarose beads (GIBCO BRL, Gaithersburg, MD) or protein A–Affiprep beads (Bio Rad Laboratories, Hercules, CA) at 25°C in IP buffer (20 mM Tris-HCl, pH 7.9, 75 mM KCl, 0.5 mM Na_3 EDTA, 0.5 mM Na_3 EGTA, 8% sucrose). Approximately 100 μg of antibody was added per 0.8 ml (packed volume) of resin. The remaining procedures were performed at 0–4°C. The beads were washed with IP buffer and incubated batchwise for 1–1.5 h with 50 ml HSS (see above). The beads were washed three times with 20 vol IP buffer containing 400 mM KCl, poured into a column, and then washed twice with elution buffer (20 mM Hepes, pH 7.5, 75 mM KCl, 0.5 mM Na_3EDTA, 0.5 mM Na_3EGTA, and 8% sucrose). The bead suspension was poured into a column and drained by gravity. One column volume of elution buffer containing 300 μg/ml KEKK peptide was added, allowed to drain by gravity, and the column was stoppered and incubated at 4°C overnight (10–16 h). The column was then eluted with several column volumes of elution buffer containing 300 μg/ml KEKK peptide. The majority of the protein eluted in the first two column volumes and contained ~100 μg total septin complex. To concentrate the protein for nucleotide analysis and NEPHGE, polyethylene glycol (PEG; mol wt = 8,000) was added to 3%. The protein was incubated for 15 min and then sedimented 100,000 rpm for 15 min in a rotor (TL100 or TL100.4; Beckman Instruments, Palo Alto, CA).

Protein Quantitation

Protein concentrations were estimated by densitometry of SDS-PAGE gels that had been stained with 0.25% Coomassie blue R-250 in 45% methanol, 10% acetic acid, then destained in 25% methanol, 7% acetic acid, followed by drying down onto cellophane membranes (Bio Rad), using a scanner and Adobe Photoshop (Adobe Systems Inc., Mountain View, CA). A standard curve was measured on the same gel using tubulin and BSA standards. Bound stain increased linearly with amount of protein per gel band over the range used (50–3,000 ng). The amount of dye absorbed per microgram of protein varies with amino acid composition, so the accuracy of this method is in the ±30% range, similar to that of Coomassie blue binding assays in solution.

To estimate the amount of Pnut polypeptide in the original high speed supernatant, we did a series of small-scale immunoprecipitations on protein A beads, keeping the amount of resin and extract constant while gradually increasing the amount of antibody on the beads until a plateau of immunoprecipitated complex was reached and the supernatant was depleted. The immunoprecipitates were quantitated by the method described above. We found that 1 ml of HSS contained ~1 μg of Pnut polypeptide. This supernatant contained 8 mg/ml of total protein, as determined by the Bradford reagent. We therefore estimate that the Pnut polypeptide is ~0.01% of the soluble protein.

Sucrose Gradient Centrifugation

After elution from the antibody column, the septin preparation was concentrated approximately fivefold using a spin concentrator (Centricon 30; Amicon, Beverly, MA), and 75 μl was loaded onto a 8–40% sucrose gradient and spun for 8 h at 55,000 rpm in a Beckman TLS-55 rotor. At the same time, 100 μl of a total embryo extract (as described above without the high speed centrifugation step), 50 ml of immunoisolated septin complex combined with protein standards, and protein standards alone were loaded onto separate parallel gradients. The mixture of septin complex and protein standards (thyroglobulin, 19.4 S; catalase, 11.3 S; aldolase, 7.3 S; and BSA, 4.5 S) allowed for a direct comparison of S values.

Gel Filtration

For gel filtration chromatography, the septin preparation was eluted from the antibody column and sedimented at 80,000 rpm for 15 min in a Beckman TL100.3 rotor. The supernatant (0.5 ml) was loaded through a guard

1. *Abbreviations used in this paper*: GST, glutathione S-transferase; HSS, high speed supernatant; PEG, polyethylene glycol; TLC, thin-layer chromatography.

column specified by the manufacturer onto a 24-ml prepacked Superose 6 HR 10/30 column (Pharmacia Fine Chemicals, Piscataway, NJ). The column had been preequilibrated with 20 mM Hepes, pH 7.5, 75 mM KCl, 0.5 mM Na_3 EDTA, 0.5 mM Na_3EGTA, and 2% sucrose. Using a flow rate of 0.3 ml/min, 0.5-ml fractions were collected. Proteins were precipitated by the addition of TCA to 10%, incubation at 0°C for 20 min, sedimentation at 15,000 *g* for 15 min, and were then analyzed by SDS-PAGE.

HSS were chromatographed as follows. In this experiment, a more concentrated extract was prepared by homogenizing 1 g of embryos in 1 ml A buffer (50 mM sodium phosphate, pH 7.5, 100 mM NaCl, 1 mM DTT). The extract was clarified by two sequential spins in a TLA 100.3 Beckman rotor at 30,000 rpm for 10 min, followed by 100,000 rpm for 8 min, and was then passed sequentially through two Bio-Spin 6 columns (bed volume of 1 ml; Bio Rad) equilibrated in the same buffer. A 100-μl aliquot of this more concentrated supernatant was loaded onto the Superose 6 column and eluted under the same conditions descibed above. 15 μl of each fraction was separated by SDS-PAGE and then probed by Western blotting with antibodies against each of the septin polypeptides. For chromatography under high salt conditions, the concentrated extract was prepared as described above and then brought up to 1 M NaCl using the Bio-Spin columns to exchange the buffer.

The native molecular mass and Stokes radius of the septin complex (both purified and in HSS) were calculated as described by Siegel and Monty (1966), using a partial specific volume of 0.737 calculated from the sequence of each septin polypeptide. The standard proteins used and their Stokes radii were the globular proteins ovalbumin (3.4 nm), catalase (5.2 nm), and thyroglobulin (8.5 nm).

Two-dimensional PAGE

Two-dimensional gel electrophoresis was performed as described by O'Farrell et al. (1977). For the first dimension, NEPHGE was carried out using a 6-cm-long 4% acrylamide slab gel (with pH 3.5–10 ampholines) that was run at 150 volts for 2 h. This was cut into strips, equilibrated with SDS, and run on a 10% SDS-PAGE gel for the second dimension.

Electron Microscopy

Freshly isolated septin complex from the affinity matrix (still containing the elution peptide) was applied to glow discharged, carbon-coated grids directly after elution from the antibody column. After 2–5 min, the grids were rinsed in water and stained with 1% uranyl acetate in 30% ethanol for 30 s. The excess uranyl acetate was then wicked away. When testing the effect of PEG, samples were incubated on ice at least 30 min before applying to the grids.

Filament Measurement

To determine filament length, EM negatives were printed at a magnification of 3 and then digitized using Image-1 software (Universal Imaging Corp., West Chester, PA). Only straight filaments, 250–300 per grid, were measured. Since longer filaments were more apt to be curved, this resulted in an underestimation of their frequency. The positions of histogram peaks were estimated by eye and replotted. For three negatives from independent grids, the slopes were 25, 26, and 28 nm/subunit.

Nucleotide Determination Using HPLC

The septin complex was concentrated by sedimentation with or without 3% PEG . The protein was then denatured by the addition of 8 M urea, 100 mM Tris-HCl, pH 7.2, followed by heating to 100°C for 1 min. 1 mM Na_3 EDTA was included in the denaturation buffer in some runs, but it obscured the position ADP would run on the column. 1/10 of the sample was removed for protein quantitation using SDS-PAGE. The remainder was diluted with 1 vol water and filtered through a 10,000-kD cut-off spin filter unit, followed by washing through the filter with 2 vol water. The pooled filtrate was analyzed by HPLC using a 1-ml Mono Q column equilibrated in 100 mM NH_4 HCO_3 and eluted with a 100–500-mM NH_4HCO_3 gradient over 30 min at a flow rate of 1 ml/min. Peak areas were analyzed and recorded at OD_{254} using Gilson HPLC software (Gilson, Inc., Middleton, WI). Standards were a mixture of 100–1,000 pmol of ADP, ATP, GDP, and GTP run separately from the sample being analyzed.

GTP Binding, Hydrolysis, and Photo–cross-linking

An immunoaffinity-isolated septin preparation still attached to antibody beads was divided into aliquots containing 20–30 μl of beads (15–40 pmol of Pnut polypeptide) in 100 μl 50 mM KCl, 20 mM Hepes, pH 7.6, 1 mM Na_3 EGTA, 3 mM $MgCl_2$, 1 mM DTT. [α-^{32}P]GTP was added to each aliquot to 500,000 cpm/aliquot along with cold GTP to give a concentration of 2 μM. After incubation at 23°C with occasional agitation, the beads were washed by centrifugation four times in 1 ml ice-cold buffer and quenched in 30 μl of 8 M urea, 20 mM TrisCl, 5 mM Na_3EDTA, pH 7.6. 1/10 of the sample was analyzed for nucleotide by thin-layer chromatography (TLC) on PEI cellulose plates in 1.4 M LiCl. 1 nmol of cold GDP and GTP each was added to every sample as a carrier, and visualized by UV absorption. The plates were dried. Labeled GDP and GTP spots were quantitated by phosphorimaging. In parallel, the protein in each sample was analyzed by running half the sample on SDS-PAGE along with BSA standards and quantitating Pnut polypeptide by densitometry. For competition experiments, cold GTP or ATP was added to 200 μM. Minus septin control beads were prepared by coating beads with random rabbit IgG, then incubating them in embryo extract and washing as indicated in the septin immunoisolation procedure. For photo–cross-linking, aliquots of septin beads were incubated in carrier-free [α-^{32}P]GTP (3,000 Ci/mmol) for 3 h at 23°C and washed (or not) as above. Aliquots of beads as a 50% slurry in buffer containing an additional 3% 2-meraptoethanol were transfered as single drops onto parafilm in a plastic dish floating on an ice bath. The drops were irradiated for 5 min with UV light (exposed bulbs from a trans-illuminator) at a distance of 6 cm. The labeled septins were analyzed by SDS-PAGE and autoradiography.

The GTP-binding and hydrolysis and photo–cross-linking experiments were performed on a septin complex that had been eluted from beads as described above, except that each reaction contained 100 μl freshly eluted complex, equivalent to 5–20 pmol Pnut. After incubation with [α-^{32}P]GTP at 23°C, the aliquot was cooled on ice, PEG was added to 3%, and the complex was sedimented at 100,000 rpm in a Beckman TL100.4 rotor for 15 min at 4°C. The pellet was washed twice in buffer by pipetting liquid in and out of the tube. The pellet was then taken up in urea buffer and analyzed as described above. Photo–cross-linking was performed in solution without removing unbound nucleotide, followed by TCA precipitation and SDS-PAGE.

Results

The carboxyl-terminal 14 amino acids (NVDGKKEKKKKGLF) of the *Drosophila* septin polypeptide Pnut (predicted mol mass = 60 kD) was used to raise an antibody in rabbits, henceforth referred to as the KEKK antibody. This region is not conserved among the known *Drosophila* septin polypeptides. Western blot analysis and immunolocalization were used to characterize this new antibody. After affinity purification, the KEKK antibody recognized the same closely spaced doublet (apparent molecular mass = 70 kD) as did a Pnut mAb (Neufeld and Rubin, 1994) when used to probe Western blots of a *Drosophila* embryo HSS (Fig. 1 *A–C*). Previous immunofluorescence data (Fares et al., 1995; Neufeld and Rubin, 1994) showed that the septins localize to the cleavage furrow in dividing cells. Postcellularization embryos were fixed and probed with the KEKK antibody (Fig. 1 *D*) and with antibodies against anillin (Fig. 1 *E*). Anillin is an actin-bundling protein that colocalizes with myosin II in cleavage furrows and contractile domains of cytoplasm in the early embryo. This antibody provides a specific marker for contractile rings (Field and Alberts, 1995). The KEKK antigen colocalized with anillin in the cleavage furrows. It also stained the cortex of syncytial embryos, particularly in contractile regions as reported for Pnut and Sep1, a second *Drosophila* septin (data not shown).

Isolation of a Septin Protein Complex

An immunoaffinity approach based on that of Zheng et al. (1995) was used to isolate a septin protein complex. An

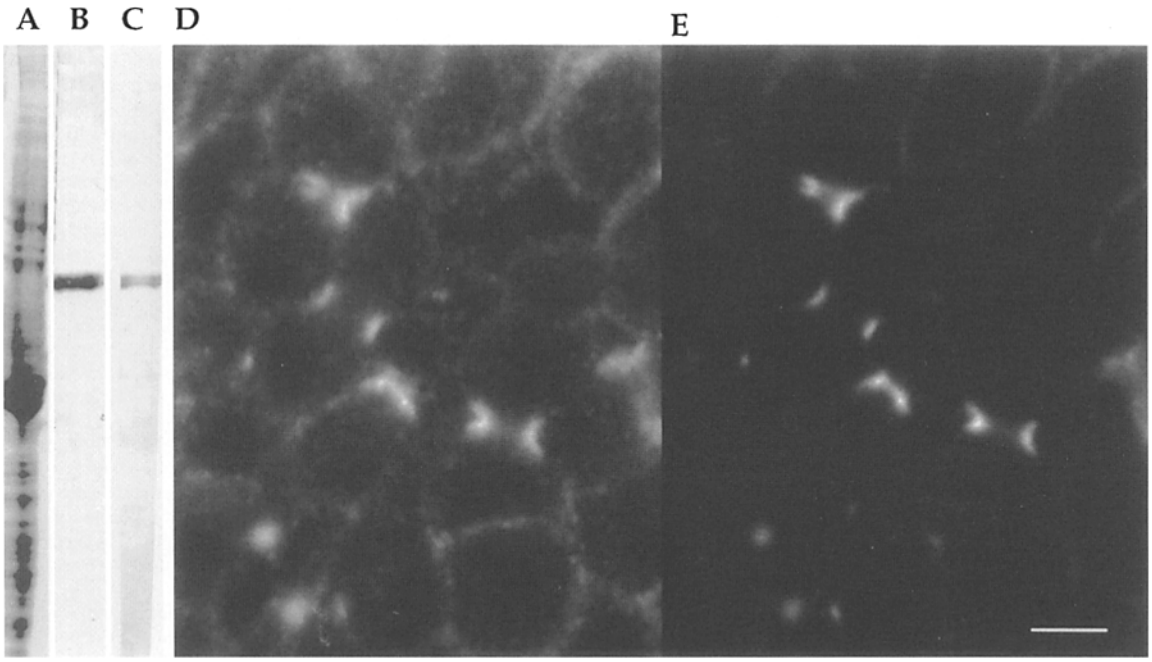

Figure 1. KEKK antibody characterization. (*A–C*) Western blot analysis. (*A*) Coomassie stain of total embryo HSS. (*B*) HSS probed with KEKK antibody. (*C*) HSS probed with 4C9, a mouse mAb against Pnut (Neufeld and Rubin, 1994). Both antibodies recognize a closely spaced doublet that migrates at ~70 kD. (*D–E*) Confocal immunofluorescence analysis of KEKK antigen localization within a mitotic domain during nuclear cycle 15. The embryo is double labeled with KEKK antibody to localize Pnut (*D*) and anti-anillin antibody (*E*). Both proteins colocalize at the cleavage furrow in dividing cells. Bar, 5 μm.

HSS was incubated with protein A beads precoated with KEKK antibody. The beads were washed in buffer containing 400 mM KCl and then eluted with KEKK peptide. This one-step purification yields a group of proteins (septin preparation) shown in Fig. 2 *A* (*SEPs*). Three polypeptides migrating with apparent molecular masses of 70, 50, and 37 kD are consistently isolated in this manner and are present in an ~1:1:1 stoichiometry. A fourth polypeptide migrating at ~23 kD was sometimes seen, but its amount varied from preparation to preparation (see also Fig. 2 *C*). The copurification of these polypeptides using an antibody specific for one of them suggests that they form a complex.

Western blot analyses (Fig. 2, lanes *PNUT*, *SEP1*, and *SEP2*) identified the three larger proteins as the known *Drosophila* septins Pnut, predicted molecular mass of 60 kD, isoelectric point 9 (Neufeld and Rubin, 1994); Sep2, predicted molecular mass of 46 kD, pI 7 (Al-Awar, O., M. Peifer, and J.R. Pringle, unpublished results) and Sep1, predicted molecular mass of 38 kD, pI 6.5 (Fares et al., 1995). The identification of the band migrating at 50 kD as Sep2 was directly confirmed by peptide sequence (data not shown). The molecular weights indicated in Fig. 2 are the apparent molecular weights from SDS-PAGE: both Pnut and Sep2 migrate as if slightly larger than their predicted molecular weights. The 23-kD band does not cross-react with any of the septin antibodies tested.

In addition to the three septin bands and the variable 23-kD band, a number of other proteins were present in substoichiometric amounts in the immunoaffinity-purified septin preparation. Additional fractionation steps were performed to test if the septins form a complex and, if so, whether other polypeptides were also components. As a first step, the septin preparation was sedimented with and without the addition of PEG. Low concentrations of PEG have a concentrating effect on proteins and can be used for selective protein precipitation from mixtures. The entire supernatant (S) and pellet (P) from a direct sedimentation (no PEG addition) are shown in Fig. 2 *B*. Note that only the three septins were present in the pellet. Addition of PEG to a final concentration of 2–3% before centrifugation increased the amount of these three septin proteins in the pellet to 90–100%. The pellet from one such experiment is shown (PEG P). As in the experiment without PEG, the 23-kD band and other minor polypeptides did not cosediment.

To test further for septin–protein association, we analyzed the immunoaffinity-purified septin preparation using sucrose gradient sedimentation and gel filtration chromatography. Polypeptides that cofractionate under these two procedures can be thought to interact in a complex. In addition, the hydrodynamic data can be used to estimate the native molecular weight and derive limited information about the shape of the complex. For sucrose gradients, the septin preparation was concentrated fivefold by ultrafiltration and then fractionated on an 8–40% sucrose gradient (Fig. 2 *D*). The three septin polypeptides cosedimented at 8 ± 0.2 S. Similarly, the three septin polypeptides eluted together from a gel filtration column in one symmetrical peak (Fig. 2 *E*) with an elution volume corresponding to an estimated Stokes radius of 9.9 nm. The 23-kD polypeptide eluted in a separate peak at a lower Stokes radius, showing that it is not part of the complex.

Unfractionated HSS from extracts of embryos were also analyzed by sucrose gradients and gel filtration. For su-

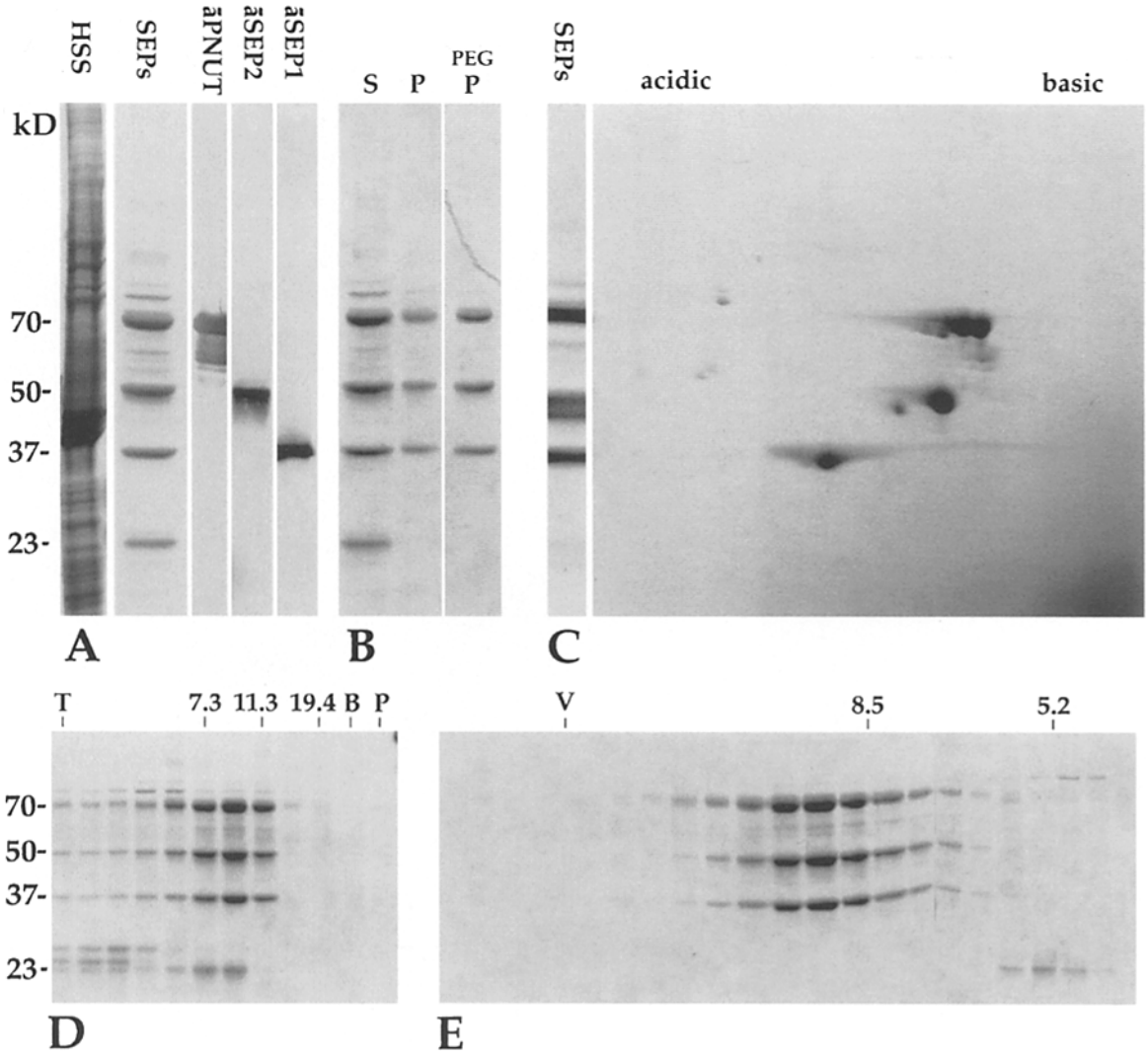

Figure 2. Biochemical analysis of the septin complex. (*A*) Identification of the components of the septin complex. *HSS*, Coomassie stain of embryo extract high-speed supernatant; *SEPs*, Coomassie stain of polypeptides eluted from the antibody/protein A beads with KEKK peptide (septin preparation). The next three lanes are Western blot analyses of the septin preparation probed with antibodies to *Drosophila* septins: anti-Pnut, anti-Sep2, and anti-Sep1, respectively. The apparent molecular weights are indicated. (*B*) Sedimentation of septin preparation as that of *A*, analyzed by SDS-PAGE, Coomassie blue staining. The first two lanes are a supernatant (*S*) and pellet (*P*) from a 10-min sedimentation at 400,000 *g*. Approximately 25% of the total septins were pelleted. This percentage varied from preparation to preparation, with a maximum of 50% of the septin polypeptides sedimenting. The lane labeled *PEG P* is the pellet from a similar sedimentation after addition of 3% PEG. (*C*) Two-dimensional NEPHGE analysis of a septin preparation (Coomassie blue stained). In this preparation, Sep2 (50 kD) migrated as a doublet on SDS-PAGE. Isolated septins (Seps) were concentrated by sedimentation in the presence of 3% PEG (as in *B*) before dissolving in two-dimensional sample buffer. (*D*) Fractionation of a septin preparation by sedimentation in an 8–40% sucrose gradient. Fractions were analyzed by SDS-PAGE and Coomassie blue staining. The three identified septin polypeptides cosedimented at 8 S. The markers are aldolase (7.3 S), catalase (11.3 S), and thyroglobulin (19.4 S). *T*, top of the gradient; *B*, bottom of the gradient; *P*, pellet. (*E*) Fractionation of a septin preparation by gel filtration chromatography. Protein eluted from the antibody column was first sedimented for 15 min at 300,000 *g*, and the resulting supernatant was then loaded onto a Superose 6 column. Fractions were analyzed by SDS-PAGE and Coomassie blue staining. The standards indicated are catalase (5.2 nm) and thyroglobulin (8.5 nm). V indicates the column void volume.

crose gradients, HSS (with and without the addition of 1 M NaCl) were run on parallel gradients and samples were analyzed by Western blotting with antibodies to all three septins. Under these conditions, the majority of the three septins cosediment at 8–8.2S, independent of salt concentration (Field, C., and O. Al-Awar, unpublished data) A similar S value (8 S) was observed when analyzing sucrose gradients of extracts with antibodies against Pnut and Sep1 (Fares et al., 1995). For gel filtration, high-speed supernatants (with and without the addition of 1 M NaCl) were chromatographed on a sizing column and analyzed by Western blotting. The elution profiles were similar to those obtained with the purified septins and had identical estimated Stokes radii (data not shown).

These data indicate that the three known *Drosophila* septin polypeptides form a stable protein complex with

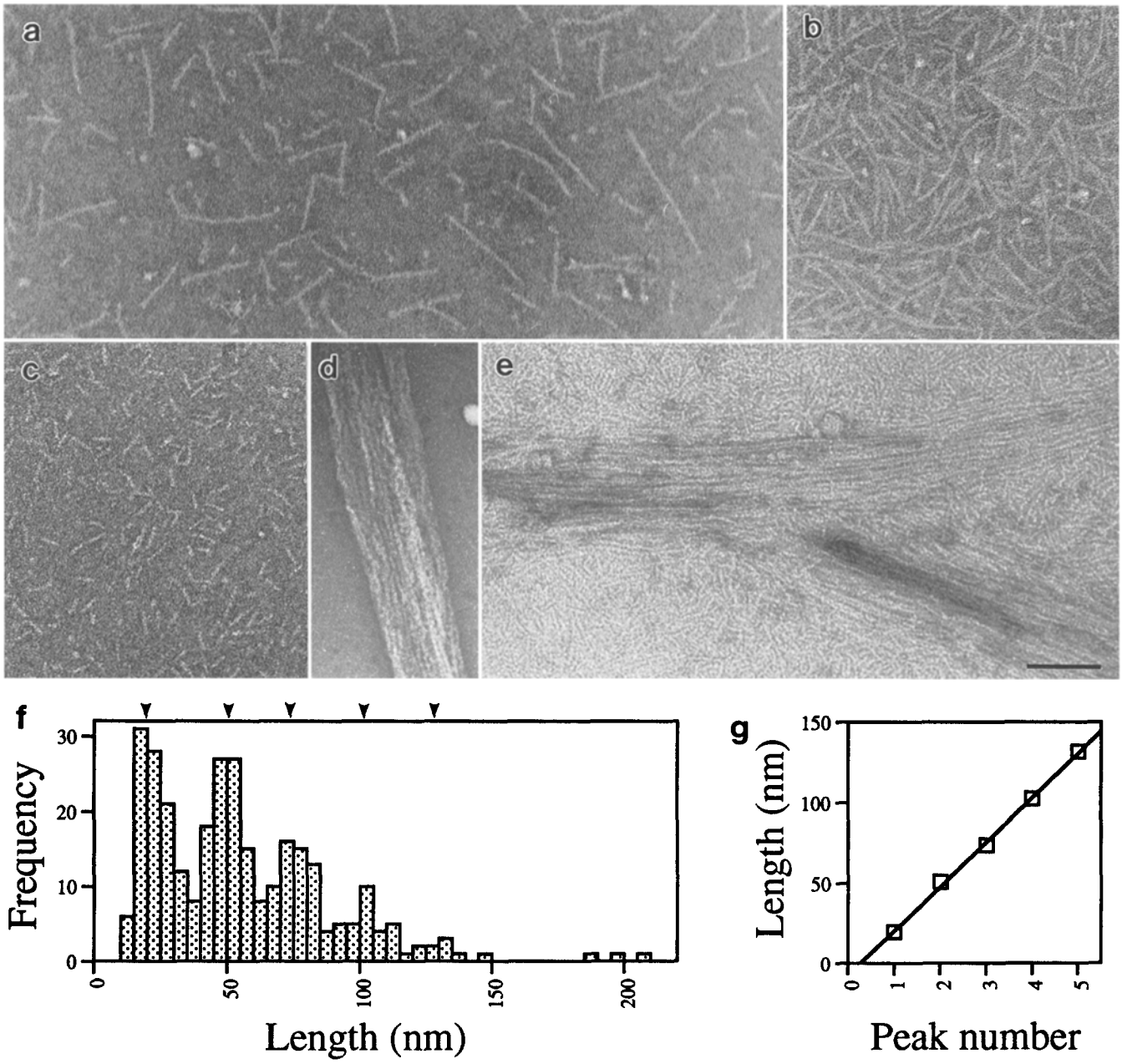

Figure 3. Negative-stain EM of septin filaments. (*a* and *b*) Typical septin preparation. Two areas where filaments have adsorbed to the grid at different densities. (*c*) A preparation diluted fivefold in elution buffer before absorption to the grid. (*d*) Part of a cable-like aggregate seen more frequently in preparations of higher protein concentration. (*e*) Filament aggregate formed by the addition of PEG to a final concentration of 1.5%. Bar, 100 nm. (*f*) Histogram of length measurements from the sample shown in *a*. Arrow indicate histogram peaks. (*g*) Plot of the peaks from the histogram shown in *f*.

similar hydrodynamic properties in both embryo extracts and purified preparations. Combining the sucrose gradient and gel filtration data using the method of (Siegel and Monty, 1966), a native molecular mass of 340 kD was estimated for the complex. The large Stokes radius relative to the molecular weight indicates that the septin complex is highly asymmetric. Two sources of error contribute to uncertainty in this native molecular weight estimate. The first is imprecision in determining where the complex and protein standards migrate during sedimentation and gel filtration. The second and usually more significant source of error comes from nonideal behavior, leading to systematic error. One significant source of error may be the tendency for gel filtration of asymmetric proteins on Superose 6 columns to give artifactually large estimates of Stokes radius (Potschka, 1987). If the Stokes radius is an overestimate, then the true native molecular weight would be smaller by up to 30%. Recent experience in this laboratory comparing the methods used here with analytical ultracentrifugation suggest that an error estimate of ±20% is reasonable.

In budding yeast, genetic evidence indicates that there are four septins involved in filament formation. Two of

these polypeptides, cdc11p and cdc12p, have very similar predicted molecular masses (47.6 and 46.7 kD) but different isoelectric points (4.7 and 8.0). Although SDS-PAGE analysis suggested that the *Drosophila* septin complex consists of only three major polypeptides, one band on SDS-PAGE could contain two comigrating polypeptides. In fact, the Sep2 band often appeared to migrate as an equal doublet (see Fig. 2 *C*, *Seps*). Resolution of the doublet was variable, and Sep2 from a single preparation migrated as a single or double band on different gels. Both bands of the doublet were sedimentable with or without PEG addition and both were recognized by the Sep2 antibody (not shown), suggesting that they are the same polypeptide. To further explore the possible existence of a fourth polypeptide, a PEG-precipitated septin complex was analyzed by two-dimensional NEPHGE (Coomassie stained) (O'Farrell et al., 1977) As shown in Fig. 2 *C*, there was no indication of a fourth major polypeptide detectable in the isoelectric-focusing dimension. The Sep2 spot appears atypically round and, upon close examination, two faint tails can be seen streaking toward the acidic side of the gel. This suggests the presence of two polypeptides of slightly different apparent molecular weights and the same isoelectric point corresponding to the doublet. The Pnut polypeptide on the NEPHGE gel displays a pattern of closely spaced spots that are consistent with multiple post-translational modifications such as phosphorylations.

Purified Septin Complex Forms Filaments

The septin preparation, immediately after elution from the antibody column, was visualized using negative stain EM (Fig. 3, *a–e*). Filaments measuring 7–9 nm in diameter and of variable length (up to 350 nm) were consistently observed. Measurement of the filaments revealed a distribution of lengths with a periodicity of ~26 nm. The periodicity is evident in a histogram (Fig. 3 *f*) and from a plot of the histogram peaks (Fig. 3 *g*). We conclude that the filaments are constructed from the repeats of a 26-nm subunit. Since mainly straight filaments were measured, longer filaments have been underrepresented in the histogram.

When the septin preparation was diluted fivefold before adsorption to the grid, the filaments appeared to fall apart, and short filaments of ~26 nm (monomers) and 50 nm (dimers) predominated (Fig. 3 *c*). In more concentrated septin preparations, the filaments tended to associate laterally and cable-like aggregates were frequently seen (Fig. 3 *d*). This tendency was accentuated by addition of PEG to 1.5% before adsorption to the grid, where paracrystal-like aggregates were seen (Fig. 3 *e*).

Septin Complex Binds and Hydrolyzes Guanine Nucleotide

The predicted amino acid sequences of all known septin proteins contain consensus sequences for GTP binding, and GTP binding and hydrolysis is known to regulate the assembly of other protein polymers (tubulin, FtsZ). To test whether purified the septin complex contains bound nucleotide, a method developed by Rosenblatt et al. (1995) was used. The eluted septin complex was concentrated and further purified by sedimentation (with or without PEG). It was then denatured with urea. Released nucleotides were separated from protein by ultrafiltration and analyzed by HPLC ion exchange. As shown in Fig. 4, the purified septin complex contained UV-absorbing material that coeluted with GDP and GTP standards. The $OD_{254/280}$ ratios of these peaks, determined using a dual-wavelength detector in the HPLC run, were consistent with their being GDP and GTP. No ADP or ATP peaks were detected. Quantitation of this analysis is shown in Table I. On average, 1.1 mol of guanine nucleotide was released per mole of septin polypeptide, with an average GDP/GTP ratio of 2.6 This data suggests that each septin polypeptide in the isolated complex binds one molecule of guanine nucleotide tightly.

To test whether the bound guanine nucleotide exchanges with free nucleotide, septin complex attached to antibody beads was incubated with [α-^{32}P]GTP. At various time points, the beads were washed, and the bound nucleotide released from the septins was analyzed by TLC and phosphorimaging. As shown in Fig. 5 *A*, ~0.3 mol of exogenously added guanine nucleotide was bound per mole of Pnut polypeptide (0.1 mol/mol septin polypeptide, if all are exchanging equally) after 18 h at 23°C. Binding was much slower at 4°C (0.08 mol/mol after 18 h). As shown in Fig. 5 *B*, binding of exogenous nucleotide was specific for guanine nucleotide, since it was efficiently competed by the addition of cold GTP but not cold ATP, and [α-^{32}P]ATP bound much less efficiently. These results can be interpreted as an indication that exogenous GTP slowly exchanges with the tightly bound guanine nucleotide that is detected by HPLC.

Hydrolysis of the bound nucleotide was also examined. This is shown in Fig. 5 (*A* and *B*), where black symbols or bars represent diphosphates, and white symbols or bars represent triphosphates. The majority (>75%) of bound guanine nucleotide (added as GTP) was recovered as GDP, and only GDP accumulated over time (compare black squares with white diamonds in Fig. 5 *A*). Under these conditions, the unbound nucleotide in the reactions remains predominantly GTP (data not shown). This sug-

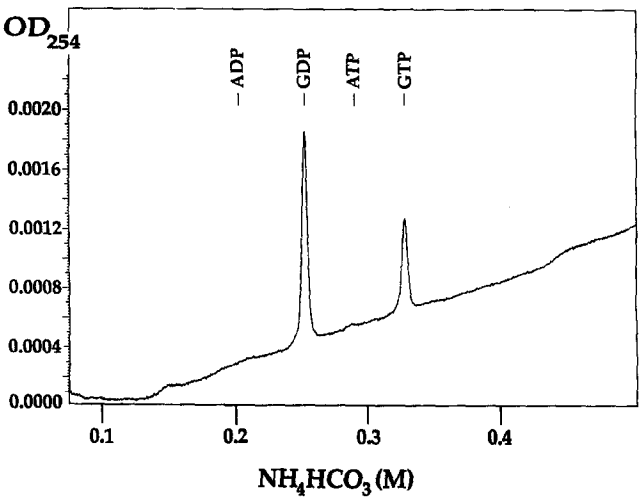

Figure 4. Analysis of nucleotides released from the purified septin complex. Nucleotides released by urea treatment were fractionated on a Mono-Q column with a gradient of NH_4HCO_3.

Table I. Analysis of Guanine Nucleotide Released from Septin Preparations by Denaturation

	Experiment 1 (PEG pellet)	Experiment 2 (PEG pellet)	Experiment 3 (PEG pellet)	Experiment 4 (pellet, no PEG)
Septin polypeptide (pmol)	59	124	370	76
GDP (pmol)	50	92	290	65
GTP (pmol)	18.5	31	124	29
GDP/GTP ratio	2.7	3.0	2.3	2.2
Guanine nucleotide/septin polypeptide ratio	1.2	1.0	1.1	1.2

Isolated septin complex (0.9–1.7 ml) was concentrated by sedimentation for 20 min at 300,000 *g* with or without addition of 3% PEG. The fraction of total septin polypeptide sedimented was >90% with PEG and 25% without PEG. After urea denaturation of the pellet, 10% was used for protein quantitation by densitometry of gels and 90% for nucleotide quantitation by HPLC using integrating software and nucleotide standards.

gests that hydrolysis is fast compared to exchange under our conditions.

Photo–cross-linking was used to determine which polypeptides bind the exogenously added guanine nucleotide. In these experiments, the purified septin preparation was incubated with [α-^{32}P]GTP, allowed to exchange for 2 h, and then irradiated with short-wavelength UV light. Irradiation was performed either before or after washing away free [α-^{32}P]GTP with similar results. The polypeptides were separated by SDS-PAGE and autoradiographed. As shown in Fig. 5 *C* (lane *1'*), radioactive GTP became covalently cross-linked predominantly to Pnut and Sep1, with Sep2 incorporating much less label. As a control, the IgG heavy chain incorporated no detectable label. This cross-linking was efficiently competed by excess unlabeled GTP (Fig. 5 *C*, lane *2'*).

The binding, hydrolysis, and cross-linking experiments with exogenous nucleotide were repeated with septins eluted from the antibody beads, using sedimentation in the presence of PEG to separate the septins from unbound nucleotide. In each case, the results were similar to those with the IgG-bound septins (data not shown). Together, the data are consistent with Pnut- and Sep1–binding guanine nucleotide tightly and undergoing slow GTP exchange followed by faster hydrolysis.

Discussion

Using immunoadsorption with an antipeptide antibody followed by elution with the peptide, we have isolated a complex of *Drosophila* septin polypeptides that bind and hydrolyze GTP and form filaments. Given their high degree of conservation, ubiquitous expression, and proven role in cytokinesis, septins are certain to be important

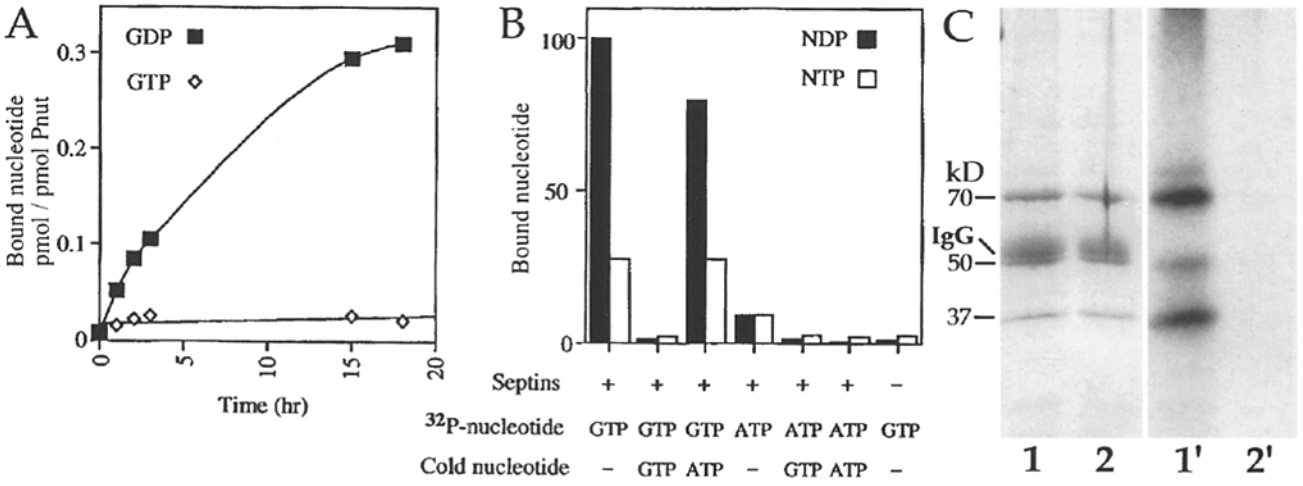

Figure 5. Nucleotide exchange and hydrolysis. (*A*) Time course of nucleotide binding and hydrolysis by the septin complex. The septin complex bound to antibody beads was incubated with 2 mM [α-^{32}P]GTP at 23°C. At various times, the beads were washed with cold buffer. Bound nucleotide was released with urea and analyzed by TLC. The majority of bound nucleotide was recovered as GDP (*black squares*). Bound nucleotide was normalized to the amount of Pnut polypeptide on the beads, measured by gel densitometry. (*B*) Specificity of nucleotide binding. The septin complex bound to antibody beads was incubated with [α-^{32}P]GTP or [α-^{32}P]ATP for 2 h at 23°C and processed as described in *A*. Random IgG beads that had been incubated in embryo extract in parallel with KEKK antibody beads were used as control (−, septins). The radioactive nucleotide and the cold competitor were added at 2 and 200 mM, respectively, as indicated. Bound nucleotide was recovered as a mixture of NDP (*black bars*) and NTP (*white bars*). (*C*) Photo–cross-linking of bound nucleotide. The septin complex bound to antibody beads was incubated with [α-^{32}P]GTP (3,000Ci/mmol) for 2 h at 23°C to allow exchange, washed in cold buffer, and irradiated with 260 nm light. Lanes *1* and *1'*, the Coomassie-stained SDS-PAGE gel and the corresponding autoradiograph, respectively. Lanes *2* and *2'*, a parallel photo–cross-linking experiment in which 200 mM cold GTP competitor was added in the initial incubation.

players in regulating cell architecture and function. The most important aspect of this work is to demonstrate for the first time that septins alone can form regular filamentous polymers, since filament formation is likely to be central to their localization and function.

Septin Complex Structure

The complex consists of three previously identified septin polypeptides, Pnut, Sep2, and Sep1, which copurify by sucrose gradient sedimentation and gel filtration chromatography. A complex of similar S value and Stokes radius exists in cytoplasmic extracts, suggesting that it is a physiologically relevant state. Combining our data with the septin amino acid sequence allows us to model the stoichiometry of the septin complex. The native molecular mass of the complex was estimated from the hydrodynamic data to be 340 kD. Densitometry of Coomassie-stained gels of the complex suggests that the three septin polypeptides are present in equimolar amounts, though potential variation in dye binding between polypeptides makes this potentially the weakest part of the data. The sum of the predicted molecular masses of the three septin polypeptides is 142 kD. Our native molecular weight estimate is closer to twice this value than it is to three times this value, so a model in which the complex contains two of each polypeptide is most consistent with our data, though we cannot rule out other possibilities. The lengths of the predicted coiled-coil domains in the three septin polypeptides are different (Pnut 89 amino acids, Sep2 74 aa, Sep1 36 aa, using the algorithm of Lupas et al., 1991). Assuming each polypeptide forms a coiled-coil, this length difference makes it most likely that each forms a homodimer. Taken together, the data best fit a model in which the complex is a heterotrimer of septin homodimers. Definitive description of the subunit stoichiometry will require higher resolution structural data.

More speculatively, we can discuss likely structures for the complex. The subunit length of the septin filaments observed by EM was 26 ± 2 nm. The Stokes radius and highly asymmetric nature of the unpolymerized complex are consistent with an elongated structure. The additive length of the three coiled-coil domains in the complex is 199 amino acids. Assuming a length of 0.14 nm/amino acid for a coiled-coil (O'Shea et al., 1991), the additive length of these three domains is 28 nm, similar to the observed subunit length. This leads to a preliminary model for the unpolymerized septin complex as a trimer of coiled-coil homodimers joined end-to-end with some overlap (Fig. 6 *A*). The GTP-binding domains in this model project out sideways, giving the polymer its width. We further speculate that these subunits associate end-to-end in a polar fashion to generate the filament (Fig. 6 *B*).

The total length of the predicted coiled-coil regions of the three *Drosophila* septins (199 amino acids) is similar to that of the predicted coiled-coil regions of the three *Saccharomyces cerevisae* neck filament–associated septins cdc3p, cdc11p, and cdc12p (201 amino acids). Thus, according to our structural model, the length of the *Drosophila* and yeast complexes would be similar. The other yeast neck filament–associated septin, cdc10p, does not contain predicted coiled-coil. Genetic studies indicate that this septin participates in neck filament formation. Perhaps the lack of a coiled-coil domain means it is not a structural component of the yeast counterpart of the heterotrimeric complex. This might explain why we see only three septins in our isolated *Drosophila* complex.

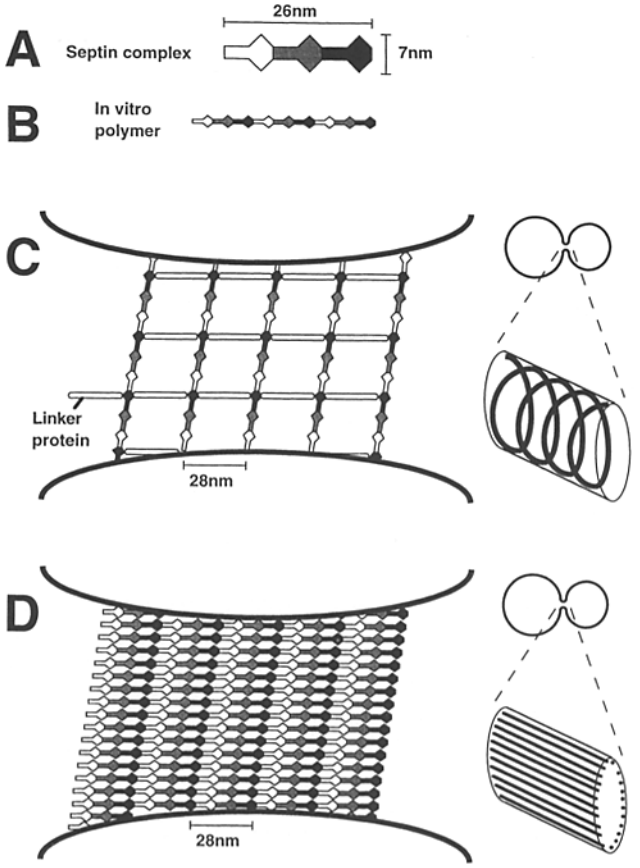

Figure 6. Models for septin filament organization. (*A*) The septin complex modeled as an end-to-end trimer of coiled-coil homodimers ~26 nm long. The heterotrimer nature of this complex is indicated by the shading of the individual homodimers. (*B*) The subunit in *A* undergoes linear polymerization to form septin filaments. (*C*) One possible arrangement of septin filaments in the yeast mother-bud neck (circumferential alignment). The image on the left shows a surface view. It is drawn to be comparable to Fig. 2 *C* in Byers and Goetsch (1976), with the mother-bud axis horizontal. The 28-nm periodicity between filaments is provided by a hypothetical linker protein. The image on the right is a perspective view illustrating the helical, circumferential arrangement of the filaments. (*D*) An alternative filament arrangement (axial-alignment). In this model, the filaments are aligned parallel to the mother bud neck, contacting each other by lateral interactions. The 28-nm periodicity is now provided by the subunit repeat. The array would appear as a circumferential filament in EM if one part of the complex (shown in black) picked up more stain, e.g., because of interaction with another protein. In the cartoon, we have oriented neighboring filaments in a parallel fashion, giving the whole array a net polarity. Antiparallel alignment might also be consistent with the EM images.

What Controls Filament Polymerization?

The septin filaments were distributed in length between 1 and 14 subunits long. This suggests a simple linear poly-

merization in which the subunits associate end-to-end with an association constant that is independent of polymer length (Fig. 6 *B*). In principle, this association constant could be derived from the length distribution (Cantor and Schimmel, 1980), but this would require a more accurate determination of filament length distributions than we have done in Fig. 3 *e*. Simple linear polymerization make the septins different from the cytoskeletal polymers actin and tubulin, which undergo nucleated polymerization, so that longer chains (past the nucleation point) grow at the expense of less stable smaller chains. A nucleation requirement or its absence has important implications for the regulation of protein polymerization in vivo, since nucleation can play a key role in controlling the spatial distribution of polymer (for example see Mitchison, 1992). If the septin polymers associate laterally with each other or with other proteins (Fig. 6, *C* and *D*), the whole assembly would likely show nucleated polymerization behavior even if the individual filaments do not, allowing for more precise spatial localization.

It is not clear at which stage in our preparation the septin complex polymerizes, and we should emphasize that we do not yet have biochemical control of polymerization in vitro. We suspect that the polymers form on the antibody beads or during the elution step, perhaps as a result of local high concentration. However, polymers could preexist in our HSS of embryo extract and, as a result of dilution, fall apart during the sucrose gradient and gel filtration procedures. We see little evidence for large complexes when HSS of embryo extracts are analyzed by sucrose gradient sedimentation or gel filtration. Approximately 50% of the Pnut polypeptide pellets during the first 10,000 *g* spin in our preparation, which suggests a polymeric state or membrane association. However, more than half the pelleted Pnut can be extracted by washing the first pellet in homogenization buffer. In preliminary experiments, the fraction of Pnut that was soluble after the first spin did not vary greatly with the extract buffers used for homogenization or with the presence of detergent. Thus, we cannot infer the state of the septins before homogenization. *Drosophila* embryos presumably contain a large store of septins to support the rapid early cell cycles, and different fractionation results might be obtained with somatic cells.

None of the conditions tested so far have resulted in an obvious increase in the polymerization state of the isolated complex, though addition of PEG does promote lateral association and sedimentability. Developing a quantitative assay for polymerization will be necessary to pursue this issue further. Potential regulators of septin polymerization in vivo include bound guanine nucleotide (discussed below), phosphorylation (or other modifications) of the septin polypeptides, and interaction with other proteins. Our two-dimensional gel analysis suggests that the Pnut polypeptide is posttranslationally modified, perhaps by phosphorylation (see Fig. 2 *C*). Phosphorylation is known to regulate the polymerization of other proteins that contain coiled-coil domains, including intermediate filaments (Heald and McKeon, 1990) and myosin II (Egelhoff et al., 1993).

GTP Binding and Hydrolysis

The isolated septin complex copurifies with one molecule of guanine nucleotide per polypeptide. Assuming the trimer of dimers structure, the complex contains four to five molecules of GDP and one to two molecules of GTP. Exogenous GTP incorporates slowly into the complex, presumably by an exchange reaction. Exchange is predominantly on Pnut and Sep1, as assayed by photo–cross-linking, and it is followed by hydrolysis. Thus, the GTP that copurifies with the complex is most likely bound to the Sep2 polypeptide.

The GTP exchange and hydrolysis kinetics of the septin complex were difficult to measure accurately because of the very slow exchange and faster hydrolysis rates. This type of exchange and hydrolysis kinetics is typical for members of the GTPase superfamily (Bourne et al., 1991). All known septin sequences have in common some of the consensus sequences that define the GTPase superfamily (Flescher et al., 1993; Nakatsuru et al., 1994). Thus the septins should be considered new members of the GTPase superfamily. By analogy to other members, we expect that GTP binding and hydrolysis will regulate the interaction of the septins with each other and/or with other proteins. Furthermore, we expect that other proteins will promote nucleotide exchange and possibly regulate hydrolysis activity, and thus regulate the location and function of the septins in vivo. One possible role for GTP binding and hydrolysis by septins is to regulate their interaction with plasma membrane receptors, and another is to regulate interactions between septin subunits during polymerization or lateral association.

GTP binding and hydrolysis is known to regulate the polymerization of tubulin and FtsZ (Mukherjee and Lutkenhaus, 1994; reviewed in Erickson, 1995), prompting speculation that septins might share biochemical mechanisms of regulation or function with these polymerizing proteins. However, tubulin and Ftsz are thought to bind GTP through related binding sites that are different from the GTPase superfamily binding sites, at least at the level of consensus motifs. Thus, while the localization of septins in yeast and FtsZ in bacteria appear similar at the light microscopic level and both proteins are involved in septation, there is currently no basis for suggesting a conserved biochemical function.

Septin Filaments In Vivo

What is the evidence that the septin polymers we saw in vitro are physiologically relevant? The filaments had a reproducible appearance and subunit repeat and have always dominated the appearance of concentrated septin complex preparations when viewed by EM. Thus, the polymers are biochemically robust, but do they exist in vivo? The size of the filaments would make them difficult to see in conventional thin-section EM of cells, unless they were present in organized arrays. For comparison, single actin filaments, which have a similar diameter, are notoriously difficult to fix and image without myosin decoration.

In *S. cerevisae*, the neck filaments were described as being 10 nm in diameter and running circumferentially in the bud neck spaced at regular 28-nm intervals. It is possible that the 7-nm filaments we observed in vitro corresponded to these 10-nm circumferential filaments, with the difference in apparent diameter accounted for by the different

EM techniques. This model is cartooned in Fig. 6 *C*. It is also possible that the filaments we see in vitro have no counterpart in vivo. We favor a third possibility, however, the axial alignment model cartooned in Fig. 6 *D*. This model orients the filaments parallel to the mother-bud neck axis, with individual filaments interacting laterally via their globular domains. The 28-nm periodicity would be provided by the septin subunit repeat. A circumferential filament appearance would be observed by EM if part of the septin complex (e.g., the polypeptide shaded in black) picked up a heavier metal stain, for example, reflecting an interaction of this polypeptide with a membrane receptor or other protein.

Both models are consistent with the available EM data, but the axial alignment model has some advantages. Regular side-to-side interaction of protein filaments naturally generates helical paths connecting laterally associated subunits, and could thus account for the appearance of both left- and right-handed helices in the mother bud neck seen by EM (for example see the discussion of microtubule lattice structure in Amos and Amos, 1991). Side-to-side interaction does not require a linker protein and may more readily accomodate the constant contraction of the animal cell cleavage furrow. In addition, our isolated septin filaments tend to associate laterally, consistent with a side-to-side association in vivo. A requirement for quasicrystalline order for visualization of the circumferential filament could explain why filaments are not seen by EM at times and places in the yeast cell cycle when the septins are localized by immunofluorescence (Ford and Pringle, 1991). We speculate that these are instances when the septins are undergoing dynamic changes. They may still be polymerized, but they lack the lateral order that is necessary to allow visualization of repeat periodicity as 10-nm filaments.

Our data leave many questions unanswered, most centrally that of septin function. The argument that the septins form the subunits of the neck filaments has been strengthened, but intriguingly, our data suggest that the circumferential filaments described by Byers and Goetsch (1976) might actually represent paths of lateral association between axially oriented filaments. Higher resolution structural data, or elongation of the coiled-coil domains by mutagenesis (Kilmartin et al., 1993), could be used to decide the orientation question. In addition, our purification sets the stage for biochemical exploration of septin function. For example, it may be possible to assay for GTP exchange or other factors that regulate polymerization or lateral aggregation. It may also be possible to use affinity methods in conjunction with different nucleotides to identify the putative membrane receptor. By combining biochemical with genetic analysis in yeast and *Drosophila*, rapid progress on septin function should be possible.

We thank the members of the Alberts lab for providing a stimulating and supportive environment in which to work. We are particularly grateful to Jack Barry, Karen Oegema, and Yixian Zheng for technical help and helpful discussions, and to Pat O'Farrell for help with interpreting two-dimensional NEPHGE gels. We are indebted to Mark Peifer, John Pringle, and members of the Pringle lab for sharing unpublished data and antibodies. We also thank Karen Oegema, John Pringle, and Yixian Zheng for critical reading the manuscript.

This work was supported by National Institutes of Health grants GM 23928 (to B.M. Alberts) and GM50868 (to J.R. Pringle and M. Peifer). M.L. Wong is supported by the Howard Hughes Medical Institute.

Received for publication 25 January 1996 and in revised form 28 February 1996.

References

Amos, L., and W.B. Amos. 1991. Molecules of the cytoskeleton. *In* Macmillan Molecular Biology Series. C. Skidmore, editor. Macmillan Education Ltd., London.

Bourne, H.R., D.A. Sanders, and F. McCormick. 1991. The GTPase superfamily: conserved structure and molecular mechanism. *Nature (Lond.)*. 349:117–127.

Byers, B. 1981. Cytology of the yeast life cycle. *In* The Molecular Biology of the Yeast *Saccharomyces*. J.N. Strathern, E.W. Jones, and J.R. Broach, editors. Cold Spring Harbor Press, Cold Spring Harbor, NY.

Byers, B., and L. Goetsch. 1976. A highly ordered ring of membrane-associated filaments in budding yeast. *J. Cell Biol.* 69:717–721.

Cantor, C., and P. Schimmel. 1980. Biophysical Chemistry Part 1: The Conformation of Biological Macromolecules. W.H. Freeman, New York.

Egelhoff, T.T., R.J. Lee, and J.A. Spudich. 1993. Dictyostelium myosin heavy chain phosphorylation sites regulate myosin filament assembly and localization in vivo. *Cell.* 75:363–371.

Erickson, H.P. 1995. FtsZ, a prokaryotic homolog of tubulin? *Cell.* 80:367–370.

Fares, H., M. Peifer, and J.R. Pringle. 1995. Localization and possible functions of *Drosophila* septins. *Mol. Biol. Cell.* 12:1843–1859.

Field, C., and B. Alberts. 1995. Anillin, a contractile ring protein that cycles from the nucleus to the cell cortex. *J. Cell Biol.* 131:165–178.

Flescher, E.G., K. Madden, and M. Snyder. 1993. Components required for cytokinesis are important for bud site selection in yeast. *J. Cell Biol.* 122:373–386.

Ford, S.K., and J.R. Pringle. 1991. Cellular morphogenesis in the *Saccharomyces cerevisiae* cell cycle: localization of the CDC11 gene product and the timing of events at the budding site. *Dev. Genet.* 12:281–292.

Haarer, B.K., and J.R. Pringle. 1987. Immunofluorescence localization of the *Saccharomyces cerevisiae* CDC12 gene product to the vicinity of the 10-nm filaments in the mother-bud neck. *Mol. Cell Biol.* 7:3678–3687.

Hartwell, L.H. 1971. Genetic control of the cell division cycle in yeast. IV. Genes controlling bud emergence and cytokinesis. *Exp. Cell Res.* 69:265–276.

Heald, R., and F. McKeon. 1990. Mutations of phosphorylation sites in lamin A that prevent nuclear lamina disassembly in mitosis. *Cell.* 61:579–589.

Kato, K. 1990. A collection of cDNA clones with specific expression patterns in the mouse brain. *Eur. J. Neurosci.* 2:704–711.

Kellogg, D.R., C.M. Field, and B.M. Alberts. 1989. Identification of microtubule-associated proteins in the centrosome, spindle, and kinetochore of the early *Drosophila* embryo. *J. Cell Biol.* 109:2977–2991.

Kilmartin, J.V., S.L. Dyos, D. Kershaw, and J.T. Finch. 1993. A spacer protein in the *Saccharomyces cerevisiae* spindle poly body whose transcript is cell cycle regulated. *J. Cell Biol.* 123:1175–1184.

Kim, H.B., B.K. Haarer, and J.R. Pringle. 1991. Cellular morphogenesis in the *Saccharomyces cerevisiae* cell cycle: localization of the CDC3 gene product and the timing of events at the budding site. *J. Cell Biol.* 112:535–544.

Koerner, T.J., J.E. Hill, A.M. Myers, and A. Tzagoloff. 1991. High-expression vectors with multiple cloning sites for construction of trpE fusion genes: pATH vectors. *Methods Enzymol.* 194:477–490.

Kumar, S., Y. Tomooka, and M. Noda. 1992. Identification of a set of genes with developmentally down-regulated expression in the mouse brain. *Biochem. Biophys. Res. Commun.* 185:1155–1161.

Longtine, M.S., D.J. DeMarini, M.L. Valencik, O.S. Al-Awar, H. Fares, C. De Virgilio, and J.R. Pringle. 1996. The septins: roles in cytokinesis and other processes. *Curr. Opin. Cell Biol.* 8:106–119.

Lupas, A., M. Van Dyke, and J. Stock. 1991. Predicting coiled coils from protein sequences. *Science (Wash. DC).* 252:1162–1164.

Miller, K.G., C.M. Field, D.R. Kellogg, and B.M. Alberts. 1991. Use of actin filament and microtubule affinity chromatography to identify proteins that bind to the cytoskeleton. *Methods Enzymol.* 196:303–319.

Mitchison, T.J. 1992. Compare and contrast actin filaments and microtubules. *Mol. Biol. Cell.* 3:1309–1315.

Mukherjee, A., and J. Lutkenhaus. 1994. Guanine nucleotide-dependent assembly of FtsZ into filaments. *J. Bacteriol.* 176:2754–2758.

Nakatsuru, S., K. Sudo, and Y. Nakamura. 1994. Molecular cloning of a novel human cDNA homologous to CDC10 in *Saccharomyces cerevisiae. Biochem. Biophys. Res. Commun.* 202:82–87.

Neufeld, T.P., and G.M. Rubin. 1994. The *Drosophila* peanut gene is required for cytokinesis and encodes a protein similar to yeast putative bud neck filament proteins. *Cell.* 77:371–379.

Nottenburg, C., W.M. Gallatin, and T. St. John. 1990. Lymphocyte HEV adhesion variants differ in the expression of multiple gene sequences. *Gene (Amst.).* 95:279–284.

O'Farrell, P.Z., H.M. Goodman, and P.H. O'Farrell. 1977. High resolution two-dimensional electrophoresis of basic as well as acidic proteins. *Cell.* 12:1133–1141.

O'Shea, E.K., J.D. Klemm, P.S. Kim, and T. Alber. 1991. X-ray structure of the GCN4 leucine zipper, a two-stranded, parallel coiled coil. *Science (Wash. DC).* 254:539–544.

Potschka, M. 1987. Universal calibration of gel permeation chromatography and determination of molecular shape in solution. *Anal. Biochem.* 162:47–64.

Pringle, J.R., R.A. Preston, A.E.M. Adams, T. Stearns, D.G. Drubin, B.K. Haarer, and E.W. Jones. 1989. Fluorescence microscopy methods for yeast. *Methods Cell Biol.* 31:357–435.

Rosenblatt, J., P. Peluso, and T.J. Mitchison. 1995. The bulk of unpolymerized actin in *Xenopus* egg extracts is ATP-bound. *Mol. Biol. Cell.* 6:227–236.

Sanders, S.L., and C.M. Field. 1994. Septins in common? *Current Biol.* 4:907–910.

Saraste, M., P.R. Sibbald, and A. Wittinghofer. 1990. The P-loop–a common motif in ATP- and GTP-binding proteins. *Trends Biochem Sci.* 15:430–434.

Sawin, K.E., T.J. Mitchison, and L.G. Wordeman. 1992. Evidence for kinesin-related proteins in the mitotic apparatus using peptide antibodies. *J. Cell Sci.* 101:303–313.

Siegel, L., and K. Monty. 1966. Determination of molecular weights and frictional ratios of proteins in impure systems by use of gel filtration and density gradient centrifugation. Application to crude preparations of sulfite and hydroxylamine reductases. *Biochim. Biophys. Acta.* 112:346–362.

Smith, D.B., and K.S. Johnson. 1988. Single-step purification of polypeptide expressed in *Escherichia coli* as fusions with glutathione S-transerase. *Gene (Amst.).* 67:31–40.

Zheng, Y., M.L. Wong, B. Alberts, and T. Mitchison. 1995. Nucleation of microtubule assembly by a γ-tubulin containing ring complex. *Nature (Lond.).* 378:578–583.